Nonlinear parametric interactions in ion-implanted semiconductor plasmas having strain-dependent dielectric constants

N Yadav[1,2], S Ghosh[1,2], and P S Malviya[1,2,†]

[1] School of Studies in Physics, Vikram University, Ujjain 465010, India
[2] Department of Physics, Govt. J.N.S. Post Graduate College, Shujalpur 465333, India

(Received 20 August 2016; revised manuscript received 27 September 2016; published online 30 November 2016)

We report nonlinear parametric interactions using a hydrodynamic model of ion-implanted semiconductor plasmas having strain-dependent dielectric constants (SDDC). High-dielectric-constant materials are technologically important because of their nonlinear properties. We find that the third-order susceptibility varies in the range 10^{-14}–10^{-12} $m^2 \cdot V^{-2}$ for ion-implanted semiconductor plasmas, which is in good agreement with previous results. It is found that the presence of SDDC in ion-implanted semiconductor plasma modifies the characteristic properties of the material.

Keywords: nonlinear parametric interactions, ion-implanted semiconductor plasmas, strain-dependent dielectric constant

PACS: 52.35.Mw, 52.77.Dq, 77.84.–s **DOI:** 10.1088/1674-1056/26/1/015203

1. Introduction

Nonlinear parametric (NLP) interactions in semiconducting materials have been studied by a number of researchers.[1–8] These interactions provide useful information regarding the physical properties of the host medium. A variety of nonlinear effects have been observed in the interaction of high-power electromagnetic waves with semiconductor plasmas.

Ion implantation is one of the most widely used doping techniques in the preparation of doped semiconductors and the manufacture of semiconductor components. The implanted ions in a material can modify the magnetic coercivity and nonlinear optical properties. A small quantity of ions may alter the electrical conductivity of the host material by several orders of magnitude. This process is responsible for implanted metal ions being neutralized as processes slow down and somehow agglomerating to form colloids. The study of the colloid formation of metal ions by ion-implanted techniques has been carried out in a number of laboratory experiments.[9] Charged grains with sizes of the order of a single micrometer exist in many laboratory, industrial, and natural plasmas. The grains are often highly negatively charged, as fast-moving thermal plasma electrons easily collide inelastically with them and become attached. The grains can be useful models for studying the structural dynamics of microscopic matter.

Crystal-like grain structures and their physical characteristics, such as melting and fracturing, have been predicted and observed in experiments and numerical simulations.[10,11]

In recent years, Ghosh and fellow researchers have reported the linear and nonlinear optical properties of nanoclusters (NCs) of implanted ions in solids. The presence of charged NCs not only modifies the wave spectrum, but also alters the amplification characteristics.[12] In the dispersion relation for slow and fast electro-kinetic waves, the charged colloids significantly modify the dispersion and absorption characteristics.[13,14] The implanted ions in group IV semiconductors agglomerate to form nano-sized grains, which can be synthesized within the host material following an appropriate annealing process. The shape and size of these grains are determined by various factors such as ion fluency and annealing treatments.[15] NLP interactions in ion-implanted semiconductor plasma are modified by the presence of non-drifting charged colloidal particles.[16]

Despite extensive research, no reports have been published on nonlinear interactions in ion-implanted semiconductor plasmas having strain-dependent dielectric constants (SDDC). Motivated by this, we examine the third-order nonlinear susceptibility of ion-implanted semiconductors having SDDC. High dielectric materials have attracted researchers because of their potential applications in microelectronics, storage memories, the miniaturization of electronic devices, and attractive physical and dielectric properties.[17] The SDDC effect for semiconductors was first observed by Pekar (in 1966) and Ogg (in 1967).[18,19] The dielectric constant is not yet fully understood. The strain dependence of the dielectric constant shows broadened peaks and considerable deviation from the Curie–Weiss-type law near critical strains; this is attributed to complete phonon softening.[20,21] The hydrodynamic model proposed in this paper for the theoretical estimation of the third-order susceptibility in ion-implanted semiconductor plasmas strikes a very good balance between accuracy and simplicity. We report the results of a numerical analysis to examine the influence of nonlinear parametric interactions

†Corresponding author. E-mail: psm_sehore@rediffmail.com
© 2017 Chinese Physical Society and IOP Publishing Ltd

in ion-implanted semiconductor plasmas on the high dielectric parameters. The analysis considers variation in the third-order susceptibility parameters of the system with the pump power, wave number, and plasma frequency in the active region.

2. Theoretical formulation

Physically, the parametric amplification of acoustic waves (AWs) is possible because of the coupling that the driving pump electric field introduces between the AW and the electron plasma wave (EPW). An acoustic perturbation in the lattice gives rise to an electron density fluctuation at the same frequency. This fluctuation couples nonlinearly with the pump electric field and drives the EPW at the sum and difference frequencies, which can be adjusted so that they are close to the electron plasma frequencies. The resulting electron density fluctuation at the plasma frequency also couples nonlinearly with an external field and can reinforce the original electron density perturbation at the acoustic frequency. Thus, under certain conditions, the AW and EPW drive each other to instability at the expense of the pump electric field.

We have considered the well-known hydrodynamic description of a homogeneous, ion-implanted n-type crystal (viz., n-$BaTiO_3$) semiconductor plasma having SDDC with electron and negatively charged colloids as carriers subjected to an electromagnetic pump wave within an external electric field (for which $k_a l \ll 1$, k_a and l being the acoustic wave number and the mean free path of an electron, respectively). Normally, the ion-implanted semiconductor plasma and its response to an applied field are treated quantum mechanically. However, in the present paper, the authors assume that the pump wave is spatially uniform and there are many photons in the field. The propagation of such a wave can be adequately described using classical mechanics.

Theoretical formulations of the third-order effective susceptibilities of electrons and colloids for ion-implanted semiconductor plasmas having SDDC have been studied previously. Nonlinear parametric interactions occur due to parametric coupling among three waves: the pump wave, acoustic wave, and scattered wave. Let us consider a spatially uniform pump electric field $E_0 \exp[\mathrm{i}(k_0 x - \omega_0 t)]$ applied to an electrostrictive field medium along the positive x-direction and parallel to the induced density modulation. We propose the following basic equations to describe the parametric interactions of the pump electric field with the medium under homogeneous ion-implanted n-type semiconductor plasma with electrons and negatively charged colloids as carriers:

$$\frac{\partial v_{0j}}{\partial t} + \upsilon_j v_{0j} = \frac{Z_j e E_0}{m_j}, \tag{1}$$

$$\frac{\partial v_{1j}}{\partial t} + \upsilon_j v_{1j} + \left(v_{0j}\frac{\partial}{\partial x}\right) v_{1j} = \frac{Z_j e E_1}{m_j}, \tag{2}$$

$$\frac{\partial n_{1j}}{\partial t} + n_{0j}\frac{\partial v_{1j}}{\partial x} + v_{0j}\frac{\partial n_{1j}}{\partial x} = 0, \tag{3}$$

$$\frac{\partial^2 u}{\partial t^2} = \frac{c}{\rho}\frac{\partial^2 u}{\partial x^2} - \frac{\varepsilon g E_0}{\rho}\frac{\partial E_1^*}{\partial x}, \tag{4}$$

$$\frac{\partial E_1}{\partial x} = \frac{n_{1j} Z_j e}{\varepsilon} + g E_0 \frac{\partial^2 u^*}{\partial x^2}, \tag{5}$$

where $j = \mathrm{e}, \mathrm{d}$ (electrons, colloids). Here, $Z_j = \frac{q_j}{e}$ is the charge state of electrons and colloids, which is the ratio of negative charges q_d that reside over the colloidal grains to the charge e on the electrons; in the further analysis, it is assumed that $Z_\mathrm{e} = -1$. Equation (1) is the momentum transfer equation, in which v_{0j} is the zero-order velocity of the carriers, denoting that the carriers will oscillate under the influence of a time-varying pump electric field. These carriers have effective mass m_j and charge $-Z_j e$. The term υ_e is the phenomenological electron collision frequency (assuming $\upsilon_\mathrm{d} \approx 0$). Similarly, equation (2) represents the first-order equation of motion for the scattered carriers with first-order fluid velocity v_{1j} due to the scattered field E_1.

Equation (3) represents the equation of continuity, in which n_0 and n_1 are the equilibrium and the perturbed carrier densities, respectively. Equation (4) describes the lattice vibration in an ion-implanted semiconductor plasma, where ρ, u, and c denote the mass density of the crystal, the lattice displacement, and the crystal elastic stiffness, respectively. The space charge field E_1 is determined by Poisson's equation (5), in which $D = \varepsilon E\,(1 + gS)$ and $\varepsilon = \varepsilon_0 \varepsilon_s$, where D is the electric displacement, ε_s is the dielectric constant in the absence of any strain $S(= \mathrm{d}u/\mathrm{d}x)$, and $g(= \varepsilon_s/3)$ is the coupling constant of the ion-implanted semiconductor plasmas having SDDC.[22]

For an electron $j = \mathrm{e}$,

$$\frac{\partial^2 n_\mathrm{e}}{\partial t^2} + \upsilon_\mathrm{e}\frac{\partial n_\mathrm{e}}{\partial t} + \omega_\mathrm{pe}^2 n_\mathrm{e} + \frac{k^2 n_{0\mathrm{e}} e g E_0}{m_\mathrm{e}} u^* = \mathrm{i}k\overline{E_\mathrm{e}} n_\mathrm{e}^*, \tag{6}$$

and for colloids $j = \mathrm{d}$,

$$\frac{\partial^2 n_\mathrm{d}}{\partial t^2} + \omega_\mathrm{pd}^2 n_\mathrm{d} + \frac{k^2 n_{0\mathrm{d}} Z_\mathrm{d} e g E_0}{m_\mathrm{d}} u^* = \mathrm{i}k\overline{E_\mathrm{d}} n_\mathrm{d}^*, \tag{7}$$

where

$$\omega_\mathrm{pe} = \left(\frac{n_{0\mathrm{e}} e^2}{m_\mathrm{e}\varepsilon}\right)^{0.5} \quad \text{and} \quad \omega_\mathrm{pd} = \left(\frac{n_{0\mathrm{d}} Z_\mathrm{d}^2 e^2}{m_\mathrm{d}\varepsilon}\right)^{0.5}$$

are the plasma frequency of electrons and colloids, respectively, and $\overline{E_\mathrm{e}} = eE_0/m_\mathrm{e}$, $\overline{E_\mathrm{d}} = Z_\mathrm{d} eE_0/m_\mathrm{d}$. We have neglected the Doppler shift under the assumption that $(\omega_0 \gg \upsilon \gg k_0 v_{0j})$. The fast component $n_{\mathrm{f}j}$ corresponds to Stokes' component of the scattered waves (SWs) and varies as $\exp[\mathrm{i}(k_1 x - \omega_1 t)]$, whereas the slow component $n_{\mathrm{s}j}$ is associated with AWs and varies like $\exp[\mathrm{i}(k_a x - \omega_a t)]$. From the above equations, we obtain the following coupled wave equation under the rotating wave approximation. For electrons,

$$\frac{\partial^2 n_\mathrm{fe}}{\partial t^2} + \upsilon_\mathrm{e}\frac{\partial n_\mathrm{fe}}{\partial t} + \omega_\mathrm{pe}^2 n_\mathrm{fe} + \frac{k^2 n_{0\mathrm{e}} e g E_0}{m_\mathrm{e}} u^* = \mathrm{i}k\overline{E_\mathrm{e}} n_\mathrm{se}^*,$$

$$\frac{\partial^2 n_{\rm se}}{\partial t^2}+\upsilon_{\rm e}\frac{\partial n_{\rm se}}{\partial t}+\omega_{\rm pe}^2 n_{\rm se}={\rm i}k\overline{E_{\rm e}}n_{\rm fe}^*. \tag{8}$$

Similarly for colloids,

$$\begin{aligned}&\frac{\partial^2 n_{\rm fd}}{\partial t^2}+\omega_{\rm pd}^2 n_{\rm fd}+\frac{k^2 n_{0\rm d}Z_{\rm d}egE_0}{m_{\rm d}}u^*={\rm i}k\overline{E_{\rm d}}n_{\rm sd}^*,\\&\frac{\partial^2 n_{\rm sd}}{\partial t^2}+\omega_{\rm pd}^2 n_{\rm sd}={\rm i}k\overline{E_{\rm d}}n_{\rm fd}^*.\end{aligned} \tag{9}$$

These equations exhibit the coupling between the low- and high-frequency components of the density perturbation $n_{\rm se}$, $n_{\rm sd}$, and $n_{\rm fe}$, $n_{\rm fd}$ via the pump electric field. Thus, the presence of the pump electric field is fundamental for the parametric interaction to occur, whereas the presence of colloids modifies the existing nonlinearities in the medium. From Eqs. (8) and (9), we can use the wave approximation to obtain the slow component $n_{{\rm s}j}^*$ for electrons and colloids as

$$\begin{aligned}n_{\rm se}^* &= -\frac{n_{0\rm e}k^2\varepsilon g^2E_0^*E_1}{\rho\left(\omega_{\rm a}^2-k_{\rm a}^2v_{\rm a}^2\right)}\\&\quad\times\left[1-\frac{\left(\delta_1^2-{\rm i}\omega_1\upsilon_{\rm e}\right)\left(\delta_2^2+{\rm i}\omega_{\rm a}\upsilon_{\rm e}\right)}{k^2\left|\overline{E_{\rm e}^2}\right|}\right]^{-1},\end{aligned} \tag{10}$$

$$n_{\rm sd}^* = -\frac{n_{0\rm d}k^2\varepsilon g^2E_0^*E_1}{\rho\left(\omega_{\rm a}^2-k_{\rm a}^2v_{\rm a}^2\right)}\left[1-\frac{\Delta_1^2\Delta_2^2}{k^2\left|\overline{E_{\rm d}^2}\right|}\right]^{-1}, \tag{11}$$

where $\delta_1^2=\left(\omega_{\rm pe}^2-\omega_1^2\right)$ and $\delta_2^2=\left(\omega_{\rm pe}^2-\omega_{\rm a}^2\right)$, $\Delta_1^2=\left(\omega_{\rm pd}^2-\omega_1^2\right)$ and $\Delta_2^2=\left(\omega_{\rm pd}^2-\omega_{\rm a}^2\right)$, and $v_{\rm a}=(c/\rho)^{0.5}$ is the acoustic velocity in the crystal medium. With a view to studying the contribution to the nonlinear current density due to the induced polarization in the medium, the effect of the transition dipole moment has been neglected. Thus, the resonant components of the induced nonlinear current due to density perturbations oscillating at the acoustic frequency are $J_j(\omega_{\rm a})=n_{{\rm s}j}^*Z_jev_{0j}$. Substituting for $n_{{\rm s}j}^*$ in the above relation and treating the induced polarization for electrons and colloids (P_j) as the time integral of the current density (J_j), we obtain $P_j=\int J_j{\rm d}t=\frac{J_j}{-{\rm i}\omega_{\rm a}}$. This leads to

$$\begin{aligned}P_{\rm e}(\omega_{\rm a}) &= \frac{k^2\varepsilon^2g^2\omega_{\rm pe}^2E_0^*E_0E_1}{\omega_0\omega_{\rm a}\rho\left(\omega_{\rm a}^2-k_{\rm a}^2v_{\rm a}^2\right)}\\&\quad\times\left[1-\frac{\left(\delta_1^2-{\rm i}\omega_1\upsilon_{\rm e}\right)\left(\delta_2^2+{\rm i}\omega_{\rm a}\upsilon_{\rm e}\right)}{k^2\left|\overline{E_{\rm e}^2}\right|}\right]^{-1},\end{aligned} \tag{12}$$

$$P_{\rm d}(\omega_{\rm a}) = \frac{k^2\varepsilon^2g^2\omega_{\rm pd}^2E_0^*E_0E_1}{\omega_0\omega_{\rm a}\rho\left(\omega_{\rm a}^2-k_{\rm a}^2v_{\rm a}^2\right)}\left[1-\frac{\Delta_1^2\Delta_2^2}{k^2\left|\overline{E_{\rm d}^2}\right|}\right]^{-1}. \tag{13}$$

The induced polarization may also be expressed as

$$P_{\rm e}(\omega_{\rm a})=\varepsilon_0\chi_{\rm e}^{(3)}E_0E_0^*E_1,$$

$$P_{\rm d}(\omega_{\rm a})=\varepsilon_0\chi_{\rm d}^{(3)}E_0E_0^*E_1.$$

This leads to the corresponding third-order susceptibility $\chi_j^{(3)}$ as

$$\begin{aligned}\chi_{\rm e}^{(3)} &= \frac{k^2\varepsilon^2g^2\omega_{\rm pe}^2}{\omega_0\omega_{\rm a}\rho\varepsilon_0\left(\omega_{\rm a}^2-k_{\rm a}^2v_{\rm a}^2\right)}\\&\quad\times\left[1-\frac{\left(\delta_1^2-{\rm i}\omega_1\upsilon_{\rm e}\right)\left(\delta_2^2+{\rm i}\omega_{\rm a}\upsilon_{\rm e}\right)}{k^2\overline{E_{\rm e}^2}}\right]^{-1},\end{aligned} \tag{14}$$

$$\chi_{\rm d}^{(3)} = \frac{k^2\varepsilon^2g^2\omega_{\rm pd}^2}{\omega_0\omega_{\rm a}\rho\varepsilon_0\left(\omega_{\rm a}^2-k_{\rm a}^2v_{\rm a}^2\right)}\left[1-\frac{\Delta_1^2\Delta_2^2}{k^2\left|\overline{E_{\rm d}^2}\right|}\right]^{-1}. \tag{15}$$

Equations (14) and (15) collectively represent the third-order susceptibility for electrons and negatively charged colloids in the semiconductor material. The effective susceptibility $\chi_{j.\rm eff}^{(3)}$ can be written as

$$\chi_{j.\rm eff}^{(3)}=\chi_{j\rm r}^{(3)}+{\rm i}\chi_{j\rm i}^{(3)}, \tag{16}$$

where the real part of the susceptibilities $\chi_{j\rm r}^{(3)}$ becomes

$$\begin{aligned}&\chi_{\rm e.real}^{(3)}\\&=\frac{k^4\varepsilon^2g^2}{\omega_0\omega_{\rm a}\rho\varepsilon_0\left(\omega_{\rm a}^2-k_{\rm a}^2v_{\rm a}^2\right)}\\&\quad\times\left[\frac{\omega_{\rm pe}^2\left|E_{\rm e}^2\right|\left(k^2\left|E_{\rm e}^2\right|-\delta_1^2\delta_2^2-\omega_1\omega_{\rm a}\upsilon_{\rm e}^2\right)}{\left(k^2\left|E_{\rm e}^2\right|-\delta_1^2\delta_2^2-\omega_1\omega_{\rm a}\upsilon_{\rm e}^2\right)^2+\upsilon_{\rm e}^2\left(\omega_{\rm a}\delta_1^2-\omega_1\delta_2^2\right)^2}\right],\end{aligned} \tag{17}$$

$$\begin{aligned}&\chi_{\rm d.real}^{(3)}\\&=\frac{k^4\varepsilon^2g^2}{\omega_0\omega_{\rm a}\rho\varepsilon_0\left(\omega_{\rm a}^2-k_{\rm a}^2v_{\rm a}^2\right)}\left[\frac{\omega_{\rm pd}^2\left|E_{\rm d}^2\right|}{k^2\left|\overline{E_{\rm d}^2}\right|-\Delta_1^2\Delta_2^2}\right].\end{aligned} \tag{18}$$

Thus, the real part of the effective susceptibility is

$$\begin{aligned}&\left[\chi_{\rm eff.real}^{(3)}\right]\\&=\frac{k^4\varepsilon^2g^2}{\omega_0\omega_{\rm a}\rho\varepsilon_0\left(\omega_{\rm a}^2-k_{\rm a}^2v_{\rm a}^2\right)}\\&\quad\times\left[\frac{\omega_{\rm pe}^2\left|E_{\rm e}^2\right|\left(k^2\left|E_{\rm e}^2\right|-\delta_1^2\delta_2^2-\omega_1\omega_{\rm a}\upsilon_{\rm e}^2\right)}{\left(k^2\left|E_{\rm e}^2\right|-\delta_1^2\delta_2^2-\omega_1\omega_{\rm a}\upsilon_{\rm e}^2\right)^2+\upsilon_{\rm e}^2\left(\omega_{\rm a}\delta_1^2-\omega_1\delta_2^2\right)^2}\right.\\&\quad\left.+\frac{\omega_{\rm pd}^2\left|E_{\rm d}^2\right|}{k^2\left|\overline{E_{\rm d}^2}\right|-\Delta_1^2\Delta_2^2}\right].\end{aligned} \tag{19}$$

The above formula reveals that the total crystal susceptibility is influenced and modified by the presence of the implanted metal colloids. The imaginary part of the third-order susceptibility becomes

$$\chi_{\rm e.imag.}^{(3)}=\frac{\upsilon_{\rm e}k^4\varepsilon^2g^2\omega_{\rm pe}^2\left|E_{\rm e}^2\right|}{\omega_0\omega_{\rm a}\rho\varepsilon_0\left(\omega_{\rm a}^2-k_{\rm a}^2v_{\rm a}^2\right)}\left[\frac{\left(\omega_{\rm a}\delta_1^2-\omega_1\delta_2^2\right)}{\left(k^2\left|E_{\rm e}^2\right|-\delta_1^2\delta_2^2-\omega_1\omega_{\rm a}\upsilon_{\rm e}^2\right)^2+\upsilon_{\rm e}^2\left(\omega_{\rm a}\delta_1^2-\omega_1\delta_2^2\right)^2}\right], \tag{20}$$

$$\chi^{(3)}_{\text{d.imag}} = 0. \tag{21}$$

Thus, the imaginary part of the effective susceptibility is

$$\chi^{(3)}_{\text{eff.imag}} = \frac{\upsilon_{\text{e}} k^4 \varepsilon^2 g^2 \omega_{\text{pe}}^2 \left|E_{\text{e}}^2\right|}{\omega_0 \omega_{\text{a}} \rho \varepsilon_0 \left(\omega_{\text{a}}^2 - k_{\text{a}}^2 v_{\text{a}}^2\right)} \times \left[\frac{\left(\omega_{\text{a}} \delta_1^2 - \omega_1 \delta_2^2\right)}{\left(k^2 \left|E_{\text{e}}^2\right| - \delta_1^2 \delta_2^2 - \omega_1 \omega_{\text{a}} \upsilon_{\text{e}}^2\right)^2 + \upsilon_{\text{e}}^2 \left(\omega_{\text{a}} \delta_1^2 - \omega_1 \delta_2^2\right)^2}\right]. \tag{22}$$

3. Results and discussion

Numerical calculations were performed for the n-type doped semiconductor sample ($BaTiO_3$) at 77 K irradiated by 10.6 μm CO_2 laser. The following material parameters were taken as representative values: $m_{\text{e}} = 0.0145 m_0$ (m_0 being the free electron rest mass), $m_{\text{d}} = 1.67 \times 10^{-27}$ kg, $\varepsilon_s = 2000$, $\rho = 4 \times 10^3$ kg·m^{-3}, $n_{0\text{e}} = 10^{25}$ m^{-3}, $n_{0\text{d}} = 2 \times 10^{20}$ m^{-3}, $\upsilon_{\text{e}} = 5 \times 10^{11}$ s^{-1}, $\omega_0 = 1.78 \times 10^{13}$ s^{-1}, $\omega_{\text{a}} = 1.6 \times 10^{13}$ s^{-1}, $v_{\text{a}} = 2.5 \times 10^3$ m·s^{-1}. The threshold characteristics are illustrated in Fig. 1. As usual, the threshold $E_{0\text{th}}$ decreases as the wave number k increases. Initially, at $k \approx 5 \times 10^7$, the threshold pump is $E_{0\text{th}} \approx 1.56 \times 10^6$ V·m^{-1}. The threshold pump decreases abruptly with k up to $k \gg 10^9$ m^{-1}, and then decreases slowly.

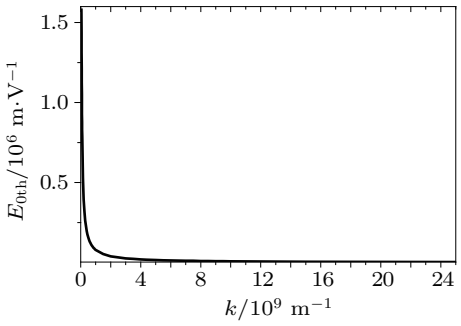


Fig. 1. Variation of threshold electric field $E_{0\text{th}}$ with wave number k.

The maximum $E_{0\text{th}}$ is found to be of order $E_{0\text{th}} \approx 10^6$ V·m^{-1}.[23] Figure 2 represents the variation of the real part of the susceptibility $\chi^{(3)}_{\text{real}}$ as a function of k at a particular pump electric field E_0 in the vicinity of the threshold $|E_{0\text{th}}|$. It can be observed that $\chi^{(3)}_{\text{real}}$ exhibits the usual dispersive characteristics of a medium with a high dielectric constant.

The real part of the acousto-optic (AO) susceptibility increases with an increase in k in the positive group velocity dispersion regime (GVD) [implying $\omega_{\text{a}}/k_{\text{a}} \approx v_\phi$ (the phase velocity of idler) $\gg v_{\text{a}}$]. The AO susceptibility shows an anomalous behavior at $k \approx 6.4 \times 10^9$ m^{-1}. However, the anomalous absorption of $\chi^{(3)}_{\text{e.real}}$ increases abruptly in the regime $\omega_{\text{a}} \approx k_{\text{a}} v_{\text{a}}$. In the negative GVD regime, $\chi^{(3)}_{\text{real}}$ abruptly increases. This can be attributed to the positive nonlinear dispersive characteristics of the medium leading to a focusing of the modulated beam. Thus, a laser propagating through an AO device operating in the negative GVD regime ($\omega_{\text{a}} \ll k_{\text{a}} v_{\text{a}}$) will have an enhanced interaction with the acoustic and scattered beams in the medium. The presence of negative charged colloids can modify the property of $\left[\chi^{(3)}_{\text{eff.real}}\right]$ (Eq. (19)). The imaginary part of the susceptibility for electrons is depicted in Fig. 3 as a function of the wave number (Eq. (20)). Initially, the curve shows that when $k_{\text{a}} v_{\text{a}} \ll \omega_{\text{a}}$ at $E_0 \approx E_{0\text{th}}$, the increase in wave number k causes the susceptibility $\chi^{(3)}_{\text{e.imag}}$ to abruptly decrease. The maximum absorption is $\chi^{(3)}_{\text{e.imag}} \approx -1.3 \times 10^{15}$ m^2·V^{-2} at $k \approx 8 \times 10^7$ m^{-1}. Beyond this point, there is a slight increase in the susceptibility and out phase when $k_{\text{a}} v_{\text{a}} = \omega_{\text{a}}$. Figure 3 shows the variation of the imaginary part of susceptibility for electron $\chi^{(3)}_{\text{e.imag}}$ with wave number k.

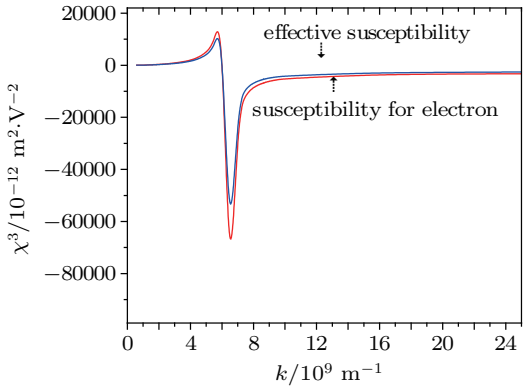


Fig. 2. (color online) Variation of the real part of susceptibility for electron $\chi^{(3)}_{\text{e.real}}$ and effective susceptibility $\left[\chi^{(3)}_{\text{eff.real}}\right]$ with wave number k.

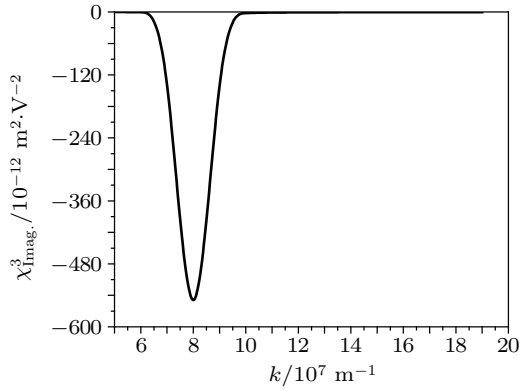


Fig. 3. Variation of the imaginary part of susceptibility for electron $\chi^{(3)}_{\text{e.imag}}$ with wave number k.

It may be inferred from Fig. 4 that, when $E_0 < E_{0\text{th}}$, both real parts of the susceptibility (the effective susceptibility and the susceptibility for electrons) are negative (which indicates absorption) and remain almost constant as E_0 increases (Eqs. (17) and (19)). However, both real parts ($\chi^{(3)}_{\text{e.real}}$ and $\chi^{(3)}_{\text{eff.real}}$) decrease and reach minima at 7×10^5 V·m^{-1} followed by a very sharp rise (amplification). The resonance peak of $BaTiO_3$ is at $\approx 8 \times 10^5$ V·m^{-1} $\approx E_{0\text{th}}$. When $k =$

1×10^8 m^{-1}, the value of $E_{0\text{th}}$ is equal to 7.89×10^5 V$\cdot$m^{-1}. Beyond this point, it decreases and becomes constant. A slight change in effective susceptibility $\chi^{(3)}_{\text{eff.real}}$ is due to the modification in the property of ion implantation in semiconductor plasmas.

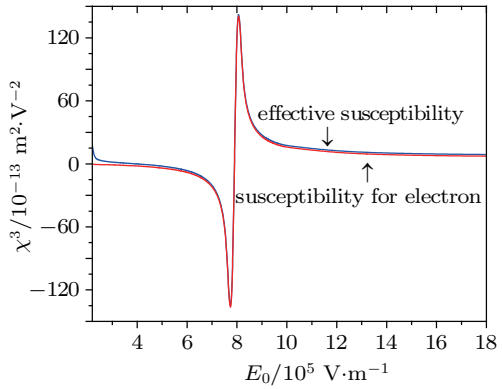


Fig. 4. (color online) Variation of the real part of susceptibility $\chi^{(3)}_{\text{real}}$ with pump electric field E_0.

The imaginary part of the susceptibility for electrons with a pump electric field is depicted in Fig. 5.

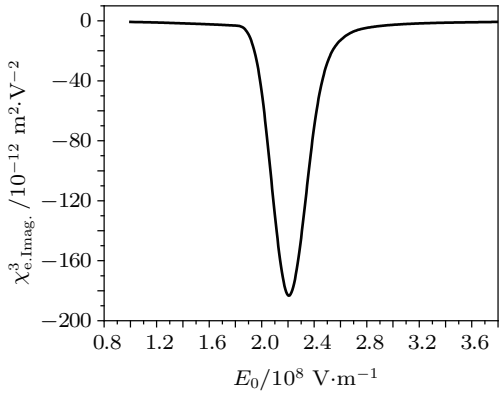


Fig. 5. Variation of the imaginary part of susceptibility $\chi^{(3)}_{\text{e.imag}}$ with pump electric field E_0.

When $E_0 \approx 2.2 \times 10^8$ V$\cdot$m$^{-1} \gg E_{0\text{th}}$ in this regime, the imaginary part of the susceptibility reaches a minimum at $\approx -1.8 \times 10^{-10}$ m$^2\cdot$V^{-2}. Initially, the curve shows the usual characteristics at $E_0 \approx 0.8 \times 10^8$ V$\cdot$m^{-1} and remains constant. The variation in the real part of the susceptibility for electrons $\chi^{(3)}_{\text{e.real}}$ as a function of carrier concentration (via ω_{pe}) is displayed in Fig. 6.

It may be inferred from Fig. 6 that, when $\omega^2_{\text{pe}} \gg \delta_1\delta_2$, the susceptibility for electrons $\chi^{(3)}_{\text{e.real}}$ can be both positive and negative. An increase in plasma frequency ω_{pe} (via the carrier concentration n_0) slowly increases the susceptibility $\chi^{(3)}_{\text{e.real}}$, which then abruptly rises with further increase in carrier concentration n_0. When $\omega_{\text{pe}} \approx 3.158 \times 10^{13}$ s^{-1} and $n_0 \approx 9.1 \times 10^{24}$ m^{-3}, the susceptibility $\chi^{(3)}_{\text{e.real}}$ changes sign, implying that the negative dispersion (absorption) characteristics further increase in the plasma frequency, causing the susceptibility to acquire negative values and saturate beyond $\left(\omega^2_{\text{pe}} \approx \delta_1\delta_2\right)$. It is evident from Eq. (17) that $E_{0\text{th}}$ reduces appreciably with an increase in carrier concentration n_0. Hence, the former is strongly dependent upon the latter. The real part of the susceptibility for colloids as a function of the plasma frequency for colloids ω_{pd} (via the carrier concentration $n_{0\text{d}}$) is depicted in Fig. 7. This figure shows the same characteristics as Fig. 6. Initially, when $\omega_{\text{pd}} \gg \Delta_1\Delta_2$, the susceptibility for colloids $\chi^{(3)}_{\text{d.real}}$ can be both negative and positive. An increase in the plasma frequency for colloids ω_{pd} (via the carrier concentration $n_{0\text{d}}$) slowly increases the susceptibility $\chi^{(3)}_{\text{d.real}}$ before there is an abrupt increase for further increases in carrier concentration $n_{0\text{d}}$.

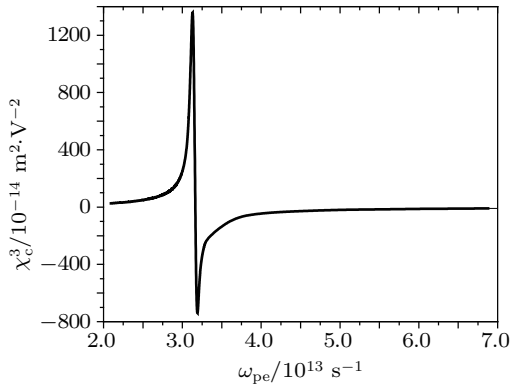


Fig. 6. Variation of the real part of susceptibility $\chi^{(3)}_{\text{e.real}}$ with plasma frequency ω_{pe}.

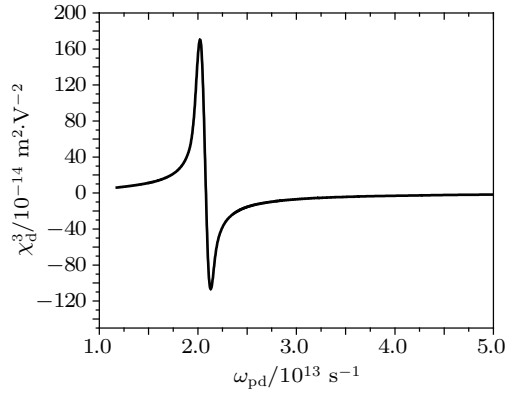


Fig. 7. Variation of the real part of susceptibility for colloids $\chi^{(3)}_{\text{d.real}}$ with plasma frequency for colloids ω_{pd}.

When $\omega_{\text{pd}} \approx 2.071 \times 10^{13}$ s^{-1} and $n_0 \approx 3.1 \times 10^{20}$ m^{-3}, the susceptibility $\chi^{(3)}_{\text{d.real}}$ changes sign, attributing negative dispersion (absorption) characteristics. Any further increase in the plasma frequency causes the susceptibility to acquire negative values and saturate beyond the point $\left(\omega^2_{\text{pd}} \approx \Delta_1\Delta_2\right)$.

4. Conclusion

In the present analysis, we have studied the possibility of NLP interactions in the real and imaginary parts of

the third-order susceptibility in ion-implanted semiconductor plasmas having SDDC. The following important conclusions may be drawn. The hydrodynamic model of semiconductor plasma has been successfully applied to ion implantation in high dielectric semiconductor materials. We calculated the magnitude of the third-order susceptibility to be $\chi^{(3)} \approx 10^{-14}$ m$^2 \cdot$ V^{-2}, which is in good agreement with other results.[24,25] In this analysis of third-order susceptibility, the presence of SDDC in ion-implanted semiconductor plasma was found to modify the characteristic properties of the material.

References

[1] Sanghavi R and Ghosh S 1992 *Acoustica* **77** 31
[2] Ortmenko O L and Sevruk B B 1996 *Acta Physica Polonica A* **90** 531
[3] Yadav N and Ghosh S *Pramana-Journal of Physics* **68** 123
[4] Wang C X, Fu S S and Gu Y Z 2009 *Chin. Phys. Lett.* **26** 097804
[5] Bhajan L and Aghamkar P 2011 *Journal of Modern Physics* **2** 771
[6] Khorashadizadeh S M, Rastbood E, Zeinaddini Meymand H and Niknam A R 2013 *Phys. Plasmas* **20** 082123
[7] Vikrant J G and Mina R Z 2014 *Scientific Reports* **4** 5617
[8] Pravat Kr M 2014 *International Journal of Applied Physics and Mathematics* **4** 379
[9] Zeba I, Ch. Uzma, Jamil M, Salimullah M and Shukla P K 2010 *Phys. Plasmas* **17** 032105
[10] Wang Y, Yu M Y, Zhao J T, Wu L and Liu S 2014 *Phys. Scr.* **89** 125601
[11] Kipton B and Erik L 2014 *Phys. Rev. Lett.* **113** 017801
[12] Ghosh S and Khare P 2006 *Indian Journals of Applied Physics* **44** 183
[13] Ghosh S, Thakur P and Salimullah M 2006 *Indian Journal of Pure & Applied Physics* **44** 235
[14] Choudhary S, Nimje N, Yadav N and Ghosh S 2014 *Physics Research Internationa* **634763**
[15] Sharma G, Ghosh S and Dad R C 2014 *J. Phys.: Conf. Ser.* **534** 012058
[16] Ghosh S, Thakur P, Yadav N, Jamil M and Salimullah M 2010 *The Arabian Journal of Science and Engineering* **35** 231
[17] Yang F, Hu G, Wu We, Yang C, Wu H and Tang M 2013 *Semicond. Sci. Technol.* **28** 082001
[18] Pekar S I 1966 *Sov. Phys. JETP* **22** 431
[19] Ogg N R 1967 *Phys. Lett.* **24A** 472
[20] Zhang X, Wang J B, Li X B, Zhong L, Lou X J and Zhou Y C 2011 *J. Appl. Phys.* **109** 126102
[21] Ong P V and Lee J 2012 *J. Appl. Phys.* **112** 014109
[22] Agrawal A K and Sharma S K 1974 *J. Appl. Phys.* **45**
[23] Ghosh S and Saxena R B 1986 *Phys. Stat. Sol.* **96** 111
[24] Yang G 2001 *Chin. Phys. Lett.* **18** 1598
[25] Cid B de Araújo1, Anderson S L and Boudebs G 2016 *Rep. Prog. Phys.* **79** 036401